Cellular uptake of gold nanoparticles triggered by host-guest interactions

Jesús Mosquera,*,† Malou Henriksen-Lacey,† Isabel García,† Miguel Martínez-Calvo,§ Jéssica Rodríguez,§ José L. Mascareñas§ and Luis M. Liz-Marzán*,†,‡

†CIC biomaGUNE and Ciber-BBN, Paseo de Miramón 182, 20014 Donostia-San Sebastián, Spain

‡Ikerbasque, Basque Foundation for Science, 48013 Bilbao, Spain

§Centro Singular de Investigación en Química Biolóxica e Materiais Moleculares (CIQUS), and Departamento de Química Orgánica. Universidade de Santiago de Compostela, 15782 Santiago de Compostela, Spain

Supporting Information Placeholder

ABSTRACT: We describe an approach to regulate the cellular uptake of small gold nanoparticles using supramolecular chemistry. The strategy relies on the functionalization of AuNPs with negatively charged pyranines, which largely hamper their penetration in cells. Cellular uptake can be activated *in situ* through the addition of cationic covalent cages that specifically recognize the fluorescent pyranine dyes and counterbalance the negative charges. The high selectivity and reversibility of the host-guest recognition activates cellular uptake, even in protein-rich biological media, as well as its regulation by rational addition of either cage or pyranine.

Gold nanoparticles (AuNPs) have raised enormous interest in cell biology and biomedicine due to their unique chemical, optical and electronic properties.[1] As a consequence, AuNPs have found many applications in areas such as drug delivery,[2] optical sensing,[3] or photothermal therapy.[4] A critical aspect to further unveil novel biomedical applications of gold nanoparticles is cellular uptake. Despite numerous studies in the field, the current understanding of the factors that influence the cell internalization of nanoparticles is still quite limited. It is accepted that commonly used AuNPs are able to cross cell membranes, usually *via* endocytic pathways;[5] however the efficiency of uptake depends on the charge, as well as on NP size, shape and surface chemistry.[6] Therefore, while positively charged NPs are often efficiently internalized, negatively charged and neutral nanoparticles of similar dimensions show a significant reduction in cellular uptake.[7] However, it is important to note that when AuNPs are dispersed in biological fluids, their surface gets covered with biomolecules, mainly proteins and lipids, forming the so-called "protein corona". As a result, their properties change and AuNP uptake is significantly affected, regardless of the initial surface charge.[8]

A major, additional challenge in the area comprises the development of strategies which allow a conditional regulation of the cell internalization process using external triggers, as this might unveil new opportunities for controlled cellular interventions.[9] Although several strategies have been described to modulate solubility,[10] aggregation[11] or photophysical properties[12] of AuNPs, methods to trigger cell uptake using an external handle are essentially limited to pH-responsive AuNPs that irreversibly aggregate or become positively charged at acidic pH, thereby enhancing cell uptake.[13]

Herein we describe a supramolecular chemistry approach to control the cellular uptake of AuNPs. The work was conceived after our recent discovery that host–guest interaction between pyranine (**pyr**) and the tetrahedron-shaped cage **A**,[14] can be used to restore the cell internalization of a pre-inhibited cell-penetrating peptide.[15] We envisioned that the attachment of enough **pyr** molecules onto AuNPs might hamper their cell internalization, owing to the build-up of a high negative surface potential. Addition of the supramolecular cage **A** should switch the negative surface into positive, and induce the cellular uptake of AuNPs (**Figure 1**).

We demonstrate the validity of this approach by using small (2 nm) Au nanospheres, a type of nanoparticles that have shown promising results as drug delivery carriers and as intracellular imaging probes.[7,16] These AuNPs are small enough to provide high payload-to-carrier ratios,[17] and recent studies have also shown than such small AuNPs present low liver accumulation and favorable kidney clearance in *in vivo* studies.[18] Importantly, we also prove that a stimulus-responsive behavior of AuNPs could be accomplished even in the presence of *fetal bovine serum* (*FBS*), and that the cellular uptake can be reversibly controlled by the judicious addition of controlled amounts of either cage **A** or pyranine.

We prepared AuNPs **with an** average core size of 2 nm **(NP1),** coated with thiolated polyethylene glycol (HS-PEG2000-NH2, Mw=2,000), using a modified Brust-Schiffrin protocol (see SI).[19] This direct reduction method ensures that the surface of the resulting amino-functionalized AuNPs is uniformly covered. The anionic pyranine fluorophore was then attached to amino groups using EDC [1-ethyl-3-(3-dimethylaminopropyl) carbodiimide hydrochloride] / NHS (N-hydroxysuccinimide) chemistry in 0.1M MES [2-*N*-morpholino)ethanesulfonic acid] at pH 6.4 (see the SI). Using these conditions, analysis of pyranine content in **NP2** revealed that about 75% of the amino groups on **NP1** were modified (see SI). The reaction was monitored by zeta potential (Zp) measurements, transmission electron microscopy (TEM) and UV-vis spectroscopy (see SI).

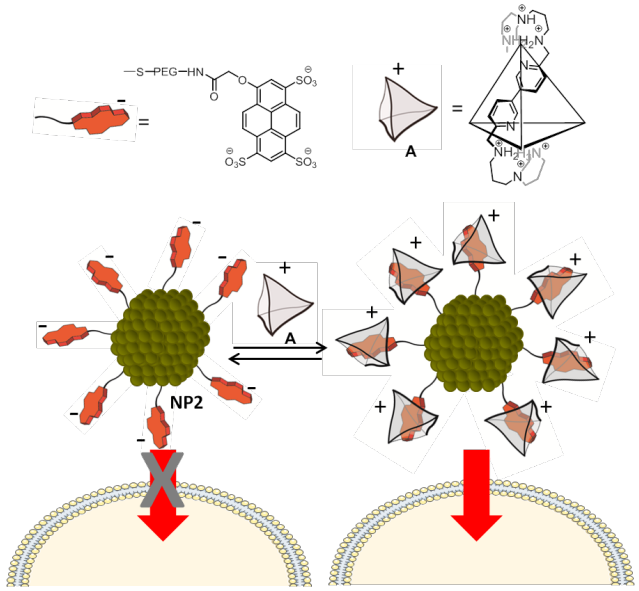

Figure 1. (Top panel) Structures of the molecular ligand pyranine and the host cage **A**. Only one edge of the tetrahedral cage is fully shown, for clarity. (Bottom panel) Schematic illustration of the approach to control the cell internalization of AuNPs by formation of supramolecular host–guest complexes between the pyranine moieties and positively charged cage **A**. PEG = poly(ethylene glycol).

As expected, **NP2** presents a negative value of Zp in aqueous solution (-15±1 mV); however, addition of cage **A** rapidly induced a shift to positive Zp. In fact, addition of only 1 μM of **A** (0.2 equiv with respect to the concentration of pyranine groups) is enough to shift the Zp of the supramolecular nanocomposite to +15±2 mV, further additions enabling a Zp up to +24 mV (**Figure S7**). These results clearly show that the interaction between pyranine and the cage switches the surface charge of the AuNPs, which remain colloidally stable.

We next investigated cell internalization of **NP2** in human HeLa cells, using the intrinsic fluorescence of the pyranine dye as a label. Cell viability assays confirmed that **NP2**, the host cage **A** and their mixture, are non-cytotoxic at the concentrations used in the subsequent microscopy studies (**Figure S8**). Interestingly, no uptake was observed after 1 h of incubation of **NP2** (80 nM, 37 ºC) in PBS (**Figure 2A**). Control experiments showed that the corrected total cell fluorescence (CTCF) in this case corresponds to cell autofluorescence. However, when the same experiment was repeated in the presence of cage **A** (5 μM), the mean value of CTCF increased up to 15-fold, thereby proving that internalization of AuNPs was very efficient under these conditions (**Figure 2B**). In fact, even after only 10 min of incubation, some intracellular fluorescence could already be observed (**Figures S9** and **S10**). Z-stacking imaging of the **NPs** in the presence of **A** further confirmed their intracellular localization (**Fig S19**). Using inductive coupled plasma - mass spectrometry (ICP-MS), we determined the average number of particles per cell after 1 h of incubation, to be 12×10^5. It is worth noting that similar results were obtained for other types of cells with different morphologies and properties, including 3T3 fibroblasts and MCF7 human lung carcinoma cells (**Figures S11 and S12**). Furthermore, NP2 analogues containing less pyranine on their surface showed the expected behavior, with NP5, having only 31%, leading to a less efficient switch (see **Figures S16-S18**).

Using an analog of the cage **A** labeled with 5-carboxytetramethylrhodamine, **A2** (see SI, page S4), [15] we found that this cage was efficiently internalized only in the presence of **NP2** (**Figure S13**). Interestingly, we found that the emission from the fluorescent cage could be co-localized with that of pyranine from NP2, after 1 h of incubation (**Figure S14**); however, co-localization between both dyes was poor after 24 h (**Figure S15**). These results suggest that both entities were uptaken together, but then the host-guest complex was disassembled and the components followed different paths. On the other hand, we repeated the uptake experiments in **Figure 2**, but in the presence of chemical inhibitors of different endocytic pathways. The results revealed that pinocytosis was the primary pathway involved in the uptake of nanoparticles carrying cage **A** (**Figure S24**).

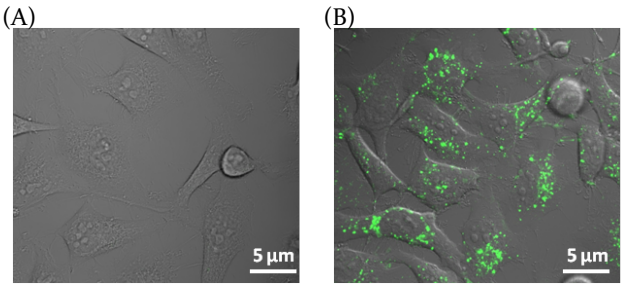

Figure 2. Fluorescence microscopy images of HeLa cells incubated with 80 nM of **NP2** at 37 ºC for 1h in PBS, after two washing steps with PBS. (A) In the absence of **A**. (B) In the presence of 5 μM of **A**.

The above results demonstrate the viability of using the supramolecular recognition events of pyranine and the oligocationic covalent cage to regulate cell uptake, and highlights the three-fold function of the pyranine moiety: fluorescent reporter, uptake inhibitor, and "convertible" handle. The efficiency of this molecule to prevent internalization is remarkable, since previous studies showed that AuNPs with similar overall negative charge can be taken up by cells.[7,20] We hypothesize that the presence of three negatively charged sulfonate groups over a rigid planar scaffold might favor electrostatic repulsion with the phospholipid membrane and thereby prevent nanoparticle uptake.

Given that incubation of NPs with cells in a complex biological fluid is known to result in protein corona formation,[8] we repeated the cell uptake experiments using DMEM *medium* with 10% *FBS*, rather than PBS. Under these conditions, and in the absence of **A**, **NP2** (80 nM) uptake was again almost negligible, even after 24 h of incubation (**Figure 3-S3**). Conversely, when the experiment was repeated in the presence of 5 μM of **A**, the cells underwent highly efficient uptake (**Figure 3-S4**). It shuld be noted that internalization under these conditions was slower than that observed when using PBS, as obtaining a similar increase in CTCF values required an incubation time of 24 h. These data confirm that the interaction between **A** and **NP2** is sufficiently strong and specific to take place even in complex biological media.

To further confirm that the effect of cage **A** is mediated by interaction with pyranines, we measured their interaction using fluorescence microscopy. In agreement with previous observations using free pyranines,[14] addition of the cationic cage to a PBS solution of **NP2** (20 nM) at room temperature, promoted a partial decrease in the fluorescence emission intensity, down to a saturation point at 4 μM of **A** (**Figure S20**). The

experiment was repeated using DMEM containing 10% *FBS* instead of PBS, and we observed the same trend, but with two differences: the initial fluorescence intensity was lower and saturation was achieved with 30 μM of the cage (**Figure S21**). These data are in agreement with the presence of a protein corona, which may quench the fluorescence of the dye and hamper the host-guest interaction. Furthermore, the higher saturation level might also be influenced by a lower availability of cage **A** in the more complex buffer.

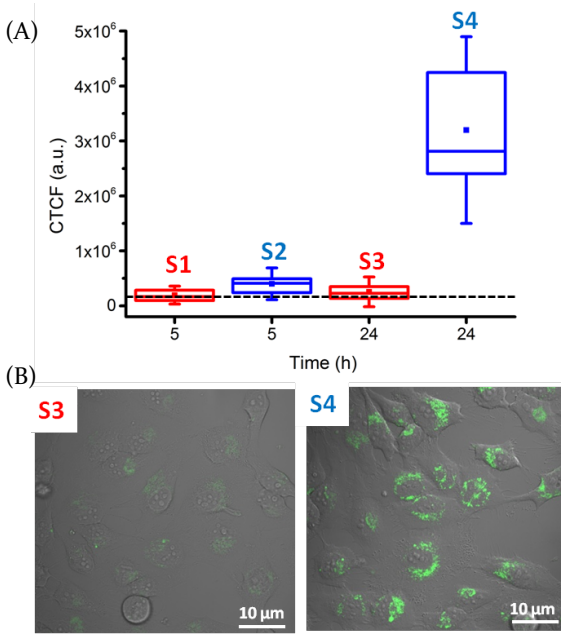

Figure 3. NP2 uptake by HeLa cells, in the presence of DMEM *medium* with 10% *FBS*. (A) CTCF variation as a function of time in the absence (red columns **S1** and **S3**) and in the presence (blue columns, **S2** and **S4**) of **A**. (B) Fluorescence micrographs for conditions **S3** and **S4** (24 h incubation in the absence and in the presence of **A**, respectively). The experiments were performed using 80 nM **NP2** at 37 ºC. The black dotted line shows the CTCF value for cellular autofluorescence. The box-and-whisker graph shows the average +/- SD with a box plot showing the 25 and 75 quartiles, and the median as a horizontal line.

Interestingly, when only 1 equiv of **pyr** (with respect to **A**) was added to a mixture of **NP2** and cage **A** (5 μM) in PBS, cell uptake was roughly halved (HeLa cells for 1 h), as compared to the same experiment in the absence of **pyr** (**Figure S22**). With this information at hand we assayed the possibility of using the capsule and **pyr** as switches to turn "on" and "off" nanoparticle uptake. As shown in **Figure 4** (see SI, for a full description of the experiment), addition of a PBS solution containing **NP2** (80 nM) to HeLa cells showed no internalization after 10 min (aka "off"). In situ addition of **A** (5 μM), and incubation for 10 min in solution resulted in a CTCF increase of ca. 2×10^5 a.u. (aka "on"). The uptake was cancelled by adding 2 equiv of free pyranine (10 μM), and restored with one more equiv of **A**, causing the CTCF to increase again (aka "on"). The uptake was cancelled again by adding two further equiv of pyranine. The switching process correlates with the expected changes in NPs surface charge (**Figure S25**). The strategy thus provides a high level of control over the cell uptake of **NP2**.

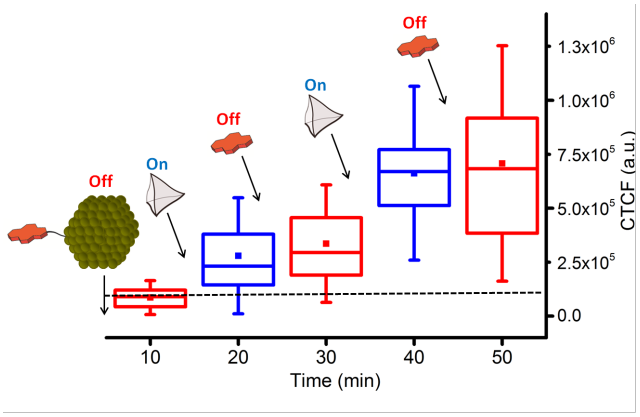

Figure 4. CTCF variation with time, upon addition of **A** and free **pyr**, based on fluorescence microscopy images of HeLa cells. Initial conditions: **NP2** (80 nM) in PBS buffer. 10 min: addition of cage **A** (5 μM). 20 min: addition of free **pyr** (10 μM). 30 min: addition of cage **A** (10 μM). 40 min: addition of of free **pyr** (20 μM). The black dotted line shows the CTCF value for cellular autofluorescence. Statistical analysis using one-way ANOVA followed by Tukey's test showed that all values are significantly different from one another, with the exception of the CTCF obtained for 20 and 30 min, and for 40 and 50 min.

In summary, we have developed a supramolecular strategy for the spatio/temporal control of the cell uptake of small gold nanoparticles, using external additives as triggers. The approach relies on the modulation of the surface charge of the nanoparticles using a Dr. Jekyll/Mr. Hide role of the pyranine moiety. AuNPs decorated with pyranines are unable to cross cell membranes, however they are efficiently internalized upon addition of an oligocationic covalent cage that interacts with pyranine, forming a positively charged host-guest complex. The methodology is compatible with complex biological media, can be used for the conditional delivery of cargoes other than pyranine and is susceptible to on/off regulation switches. Therefore, it promises to become useful for biological applications such as drug delivery and cell imaging, or other NP-mediated cellular interventions.

ASSOCIATED CONTENT

Supporting Information

The Supporting Information is available free of charge on the ACS Publications website.

Supplemental Figures S1–S25, experimental procedures, and cell studies.

AUTHOR INFORMATION

Corresponding Authors

Jesús Mosquera (jmosquera@cicbiomagune.es)
Luis M. Liz-Marzán (llizmarzan@cicbiomagune.es)

ORCID

Jesús Mosquera (0000-0001-6878-4567)
Luis M. Liz-Marzán (0000-0002-6647-1353)
José L. Mascareñas (0000-0002-7789-700X)

Notes

The authors declare no competing financial interest.

ACKNOWLEDGMENT

This work has been funded by MINECO (Grant MAT2017-86659-R and SAF2016-76689-R), the Xunta de Galicia (2015-CP082, ED431C 2017/19, and Centro singular de investigación de Galicia accreditation 2016–2019, ED431G/09), the European Regional Development Fund, and the European Research Council (Advanced Grant No. 340055). JM and MMC thank MINECO for Juan de la Cierva-fellowships (FJCI-2015-25080 and IJCI-2014-19326). The authors thank Prof. Jonathan R. Nitschke for his assistance in the synthesis of **A**.

REFERENCES

(1) (a) Langer, J.; and Novikov, S. M.; Liz-Marzán, L. M. *Nanotechnology* **2015**, *26* (32), 322001. (b) Saha, K.; Agasti, S. S.; Kim, C.; Li, X.; Rotello, V. M. *Chem. Rev.* **2012**, *112* (5), 2739. (c) Guo, L.; Xu, Y.; Ferhan, A. R.; Chen, G.; Kim, D.-H. *J. Am. Chem. Soc.* **2013**, *135* (33), 12338. (d) Amendola, V.; Pilot, R.; Frasconi, M.; Maragò, O. M.; Iatì, M. A. *J. Phys. Condens. Matter* **2017**, *29* (20), 203002.

(2) (a) Cheng, Y.; Meyers, J. D.; Broome, A.-M.; Kenney, M. E.; Basilion, J. P.; Burda, C. *J. Am. Chem. Soc.* **2011**, *133* (8), 2583. (b) Strozyk, M. S.; Carregal-Romero, S.; Henriksen-Lacey, M.; Brust, M.; Liz-Marzán, L. M. *Chem. Mater.* **2017**, *29* (5), 2303.

(3) Hu, Y.; Cheng, H.; Zhao, X.; Wu, J.; Muhammad, F.; Lin, S.; He, J.; Zhou, L.; Zhang, C.; Deng, Y.; Wang, P.; Zhou, Z.; Nie, S.; Wei, H. *ACS Nano* **2017**, *11* (6), 5558.

(4) (a) Hainfeld, J. F.; Lin, L.; Slatkin, D. N.; Dilmanian, F. A.; Vadas, T. M.; Smilowitz, H. M. *Nanomedicine Nanotechnol. Biol. Med.* **2014**, *10* (8), 1609. (b) Abadeer, N. S.; Murphy, C. J. *J. Phys. Chem. C* **2016**, *120* (9), 4691.

(5) (a) Saha, K.; Kim, S. T.; Yan, B.; Miranda, O. R.; Alfonso, F. S.; Shlosman, D.; Rotello, V. M. *Small* **2013**, *9* (2), 300. (b) Dykman, L. A.; Khlebtsov, N. G. *Chem. Rev.* **2014**, *114* (2), 1258.

(6) (a) Chithrani, B. D.; Ghazani, A. A.; Chan, W. C. W. *Nano Lett.* **2006**, *6* (4), 662. (b) Wang, X.; Hu, X.; Li, J.; Russe, A. C. M.; Kawazoe, N.; Yang, Y.; Chen, G. *Biomater. Sci.* **2016**, *4* (6), 970. (c) Xie, X.; Liao, J.; Shao, X.; Li, Q.; Lin, Y. *Sci. Rep.* **2017**, *7* (1), 3827.

(7) Jiang, Y.; Huo, S.; Mizuhara, T.; Das, R.; Lee, Y.-W.; Hou, S.; Moyano, D. F.; Duncan, B.; Liang, X.-J.; Rotello, V. M. *ACS Nano* **2015**, *9* (10), 9986.

(8) (a) Lesniak, A.; Salvati, A.; Santos-Martinez, M. J.; Radomski, M. W.; Dawson, K. A.; Åberg, C. *J. Am. Chem. Soc.* **2013**, *135* (4), 1438. (b) Cheng, X.; Tian, X.; Wu, A.; Li, J.; Tian, J.; Chong, Y.; Chai, Z.; Zhao, Y.; Chen, C.; Ge, C. *ACS Appl. Mater. Interfaces* **2015**, *7* (37), 20568.

(9) (a) Learte-Aymamí, S.; Curado, N.; Rodríguez, J.; Vázquez, M. E.; Mascareñas, J. L. *J. Am. Chem. Soc.* **2017**, *139* (45), 16188. (b) Jiang, T.; Olson, E. S.; Nguyen, Q. T.; Roy, M.; Jennings, P. A.; Tsien, R. Y. *Proc. Natl. Acad. Sci. U. S. A.* **2004**, *101* (51), 17867. (c) Bang, E.-K.; Gasparini, G.; Molinard, G.; Roux, A.; Sakai, N.; Matile, S. *J. Am. Chem. Soc.* **2013**, *135* (6), 2088.

(10) (a) Peng, L.; You, M.; Wu, C.; Han, D.; Öçsoy, I.; Chen, T.; Chen, Z.; Tan, W. *ACS Nano* **2014**, *8* (3), 2555. (b) Honold, T.; Skrybeck, D.; Wagner, K. G.; Karg, M. *Langmuir* **2017**, *33* (1), 253.

(11) (a) Liu, J.; Mendoza, S.; Román, E.; Lynn, M. J.; Xu, R.; Kaifer, A. E. *J. Am. Chem. Soc.* **1999**, *121* (17), 4304. (b) Zhao, H.; Sen, S.; Udayabhaskararao, T.; Sawczyk, M.; Kučanda, K.; Manna, D.; Kundu, P. K.; Lee, J.-W.; Král, P.; Klajn, R. *Nat. Nanotechnol.* **2016**, *11* (1), 82.

(12) (a) Hu, H.; Ji, F.; Xu, Y.; Yu, J.; Liu, Q.; Chen, L.; Chen, Q.; Wen, P.; Lifshitz, Y.; Wang, Y.; Zhang, Q.; Lee, S.-T. *ACS Nano* **2016**, *10* (8), 7323.

(13) (a) Mizuhara, T.; Saha, K.; Moyano, D. F.; Kim, C. S.; Yan, B.; Kim, Y.-K.; Rotello, V. M. *Angew. Chem. Int. Ed.* **2015**, *54* (22), 6567. (b) Liu, X.; Chen, Y.; Li, H.; Huang, N.; Jin, Q.; Ren, K.; Ji, J. *ACS Nano* **2013**, *7* (7), 6244. (c) Ding, H.; Ma, Y. *Sci. Rep.* **2013**, *3*, srep02804.

(14) Mosquera, J.; Zarra, S.; Nitschke, J. R. *Angew. Chem. Int. Ed.* **2014**, *53* (6), 1556.

(15) Rodríguez, J.; Mosquera, J.; Couceiro, J. R.; Nitschke, J. R.; Vázquez, M. E.; Mascareñas, J. L. *J. Am. Chem. Soc.* **2017**, *139* (1), 55.

(16) (a) Huang, K.; Ma, H.; Liu, J.; Huo, S.; Kumar, A.; Wei, T.; Zhang, X.; Jin, S.; Gan, Y.; Wang, P. C.; He, S.; Zhang, X.; Liang, X.-J. *ACS Nano* **2012**, *6* (5), 4483. (b) Zhou, C.; Long, M.; Qin, Y.; Sun, X.; Zheng, J. *Angew. Chem. Int. Ed.* **2011**, *50* (14), 3168.

(17) Oh, E.; Delehanty, J. B.; Sapsford, K. E.; Susumu, K.; Goswami, R.; Blanco-Canosa, J. B.; Dawson, P. E.; Granek, J.; Shoff, M.; Zhang, Q.; Goering, P. L.; Huston, A.; Medintz, I. L. *ACS Nano* **2011**, *5* (8), 6434.

(18) (a) Zhang, X.-D.; Wu, D.; Shen, X.; Liu, P. X.; Fan, F Y.; Fan, S. J. *Biomaterials* **2012**, *33* (18), 4628. (b) Frigell, J.; García, I.; Gómez-Vallejo, V.; Llop, J.; Penadés, S. *J. Am. Chem. Soc.* **2014**, *136* (1), 449.

(19) Brust, M.; Walker, M.; Bethell, D.; Schiffrin, D. J.; Whyman, R. *J. Chem. Soc. Chem. Commun.* **1994**, *0* (7), 801.

(20) Verma, A.; Uzun, O.; Hu, Y.; Hu, Y.; Han, H.-S.; Watson, N.; Chen, S.; Irvine, D. J.; Stellacci, F. *Nat. Mater.* **2008**, *7* (7), 588.

(21) (a) Settanni, G.; Zhou, J.; Suo, T.; Schöttler, S.; Landfester, K.; Schmid, F.; Mailänder, V. *Nanoscale* **2017**, *9* (6), 2138. (b) Lundqvist, M.; Augustsson, C.; Lilja, M.; Lundkvist, K.; Dahlbäck, B.; Linse, S.; Cedervall, T. *PLOS ONE* **2017**, *12* (4), e0175871.

Table of Contents artwork